Preprint: Bridgelall, R., Askarzadeh, T., and Tolliver, D. (2023). Introducing an Efficiency Index to Evaluate eVTOL Designs. *Technology Forecasting and Social Change*, 191 (122539). DOI: 10.1016/j.techfore.2023.122539

Introducing an Efficiency Index to Evaluate eVTOL Designs

Raj Bridgelall, Ph.D. (Corresponding Author)
Associate Professor
Transportation, Logistics & Finance, College of Business
North Dakota State University
PO Box 6050, Fargo ND 58108-6050
Email: raj@bridgelall.com, ORCID: 0000-0003-3743-6652

Taraneh Askarzadeh
Doctoral Graduate Research Assistant
Transportation, Logistics & Finance, College of Business
North Dakota State University
PO Box 6050, Fargo ND 58108-6050
Email: taraneh.askarzadeh@ndsu.edu, ORCID: 0000-0002-4301-8310

Denver D. Tolliver, Ph.D.
Director, Upper Great Plains Transportation Institute
North Dakota State University
PO Box 6050, Fargo, ND 58108
Email: denver.tolliver@ndsu.edu, ORCID: 0000-0002-8522-9394

Declarations of interest: none

Abstract

The evolution of electric vertical takeoff and landing (eVTOL) aircraft as part of the Advanced Air Mobility initiative will affect our society and the environment in fundamental ways. Technological forecasting suggests that commercial services are fast emerging to transform urban and regional air mobility for people and cargo. However, the complexities of diverse design choices pose a challenge for potential adopters or service providers because there are no objective and simple means to compare designs based on the available set of performance specifications. This analysis defines an aeronautically informed propulsion efficiency index (PEX) to compare the performance of eVTOL designs. Range, payload ratio, and aspect ratio are the minimum set of independent parameters needed to compute a PEX that can distinguish among eVTOL designs. The distribution of the PEX and the range are lognormal in the design space. There is no association between PEX values and the mainstream eVTOL architecture types or the aircraft weight class. A multilinear regression showed that the three independent parameters explained more than 90% of the PEX distribution in the present design space.

Keywords: Advanced air mobility; aerodynamic efficiency; multilinear regression; regional air mobility; smart cities; urban air mobility

1 Introduction

Ever since Uber, the multinational ride-hailing company, proposed using vertical takeoff and landing (VTOL) aircrafts for its on-demand urban air mobility (UAM) initiative in 2016 (Uber Elevate, 2016), there has been a proliferation of companies seeking to participate. The market opportunity for UAM stems from the desire to avoid road traffic congestion for travel between urban centers and between cities in a region. Aerospace companies see electric VTOL (eVTOL) designs as the solution because they require a relatively small footprint to take off and land, no runways, no petroleum-based refueling facilities, and they can provide easy access from existing urban facilities such as atop parking garages, tall buildings, warehouses, and underutilized heliports. The anticipation of lucrative profits from UAM has attracted big aerospace companies like Airbus, Boeing, and Bell, vehicle manufacturers like Hyundai, and scores of aerospace startups that have already raised billions of dollars in investment capital (Constantine, 2020). American Airlines, Jet Blue, and United Airlines placed aircraft preorders in 2021 to the startups known as Vertical Aerospace, Joby Aviation, and Archer Aviation, respectively (Kolodny & Josephs, 2021).

The proliferation of eVTOL designs has created a complex spectrum of performance specifications, each based on unique patented design choices. Hence, without cross-licensing agreements, it is not likely that any two eVTOL designs would be identical. There are currently two broad design categories: unwinged (multicopters) and winged (Garrow, German, & Leonard, 2021). The winged designs have five subcategories: transitioned thrust (TT), tilt rotor (TR), tilt wing (TW), folding wing (FW), and fixed rotor (FR). In general, winged architectures provide greater flight efficiency during cruise mode. Even so, there are many design variations within

each subcategory. The literature review section explores the reasons for those design choices and their various tradeoffs.

The complex design choices have created a **problem** for decision makers who wish to evaluate price and application suitability based on some objective measure of performance efficiency. Hence, the **goal** of this research is to develop a simple propulsive efficiency index (PEX) that can position *winged* eVTOL designs along a linear performance spectrum that encapsulates the most important design choices such as range, payload capacity, and footprint. Consequently, the **research questions** are:

1. What is the minimum set of independent design parameters that can define a PEX?
2. Does the PEX distribution in the existing design space follow any classic function such as the Gaussian (normal) or lognormal?
3. Is there an association between eVTOL architecture types and the PEX in the present design space?
4. Is there an association between aircraft weight and the PEX in the present design space?
5. How well do the dependent parameters of the PEX explain the distribution of the PEX in the design space?
6. How do the dependent parameters rank in their explanation of the PEX distribution in the design space?

The organization of the remainder of this paper is as follows: Section 2 conducts a literature review that covers adoption forecasting, architecture convergence, and flight range projections. Section 3 derives the formulas that govern cruise flight to inform the independent variables that make up the proposed PEX. Section 4 discusses the results in terms of the PEX distribution in the design space and the ranking of those factors that explain the distribution. Section 5

concludes the paper and offers a glimpse into future work.

2 Literature Review

Advanced Air Mobility (AAM) is an air transportation initiative for moving people and freight between places that lack service from efficient ground transportation or aviation (NAS, 2020). Passenger markets for eVTOL aircrafts will include urban air taxis, shuttles between urban and suburban areas, and flights between regional cities. Early freight applications aim to fill the gap in rural domestic cargo operations and increase the proportion of customers in a region that can get same-day delivery service. Amazon already offers one-day or same-day service to 72% of the U.S. population but endeavors to increase that proportion (NASA, 2021). The announcements of billions of dollars of investments in new eVTOL aircraft companies and the recent transition of several startups such as Archer Aviation, Joby Aviation, and eHang to publicly traded companies are evidences of the fast growing interest in Urban Air Mobility (UAM) or Advanced Air Mobility (AAM) (Cohen, Shaheen, & Farrar, 2021).

UAM/AAM-related publications in the American Institute of Aeronautics and Astronautics (AIAA) database increased from 4 in 2015 to 94 in 2019 (Garrow, German, & Leonard, 2021). The literature suggests that the year 2022 is when manufacturers will begin to focus their attention on aircraft certification and advance their roadmap to operationalization by 2030. eVTOL aircraft deployments are also underway to enable a variety of smart city initiatives (Mohamed, Al-Jaroodi, Jawhar, Idries, & Mohammed, 2020). The next subsections focus on research to forecast the addressable market, the eVTOL architecture convergence, and flight range projections.

2.1 Adoption Forecasts

Although market size estimates by seasoned research firms vary substantially, their projections

for different horizon years reveal an exponential growth. BBC Research estimated the global market for drone technology will reach $54.6 billion by 2025, with a compound annual growth rate (CAGR) of 12.7% (BBC Research, 2020). The market research firm Brandessence estimated that global drone revenue was $18.28 billion in 2020, and that revenues could reach $40.9 billion by 2027 based on an estimated CAGR of 12.27% (Brandessence, 2021). Joint research by Deloitte Consulting LLP and the Aerospace Industries Association (AIA) estimated that the U.S. market for AAM will reach $115 billion by 2035, which is equivalent to 30% of the U.S. commercial aerospace market in 2019 (Lineberger, Silver, & Hussain, 2021). Morgan Stanley estimated that the global market for autonomous aircrafts will reach $1.5 trillion by 2040 (Morgan Stanley, 2018). Ronald Berger GmbH estimated that 98,000 passenger drones will operate by 2050 in areas where they can substantially reduce the total travel time (the sum of waiting, boarding, and egress times) for distances between 9 miles (15 km) and 16 miles (25 km) (Baur, Schickram, Homulenko, Martinez, & Dyskin, 2018).

Lessons learned from the early ambitious projections of autonomous vehicle (AV) adoption suggest that resolving technical issues such as automation and enacting regulatory policies often take much longer than first anticipated (Guo, et al., 2021). Current adoption challenges include user acceptance, willingness-to-pay, seamless integration into the national airspace, and the buildout of support infrastructures such as vertiports and fast charging facilities (Lineberger, Silver, & Hussain, 2021). There are still many unresolved risks for the safe integration of drones into the national airspace system (NAS, 2018). Regulations can both promote and suppress innovation (Nakamura & Kajikawa, 2018). As the price of commercial drones plummets, more nefarious actors will be able to afford them (Ayamga, Akaba, & Nyaaba, 2021). Batteries can become more expensive because of the global lack of critical materials such

as copper, lithium, nickel, cobalt, and rare earth elements needed to meet the growing demand (IEA, 2021). The worldwide market for lithium batteries will grow by a factor of 5 to 10 by 2030, and currently only a few countries can supply those materials (FCAB, 2021). The many challenges of AAM suggest that current adoption forecasts may be too optimistic (Kellermann, Biehle, & Fischer, 2020).

Adoption will more likely occur in stages where the easiest-to-deploy applications with the greatest demand will occur first. Electric or hybrid VTOL aircrafts will initially replace conventional helicopters in many applications because of their lower cost, reduced risk from using multiple rotors, and quiet operation (Vieira, Silva, & Bravo, 2019). The emergency medical transport of human organs, blood, laboratory samples, vaccines, medicine, and first responders can more easily overcome adoption reluctance (Pulsiri & Vatananan-Thesenvitz, 2021). The near-term technical challenges of safely increasing battery energy storage density will force service providers to first focus on short-haul flights (Zheng & Rutherford, 2021). Service will likely begin from existing U.S. heliports that already support VTOL flights (FAA, 2020). There are 5,901 U.S. heliports that account for 30% of the total public and private landing spaces in the United States. This number includes 13,065 airports (FAA, 2020). The global pandemic has accelerated the testing of drones to deliver online orders, so that market segment is likely to continue its rapid growth (Yaprak, Kılıç, & Okumuş, 2021).

2.2 Architecture Convergence

The cost reduction and efficiency enhancements of electrified motors have enabled the transition from few motors to many motors distributed around the airframe. This approach, called distributed electric propulsion (DEP), has become the common design choice for eVTOL aircraft designs because it enhances safety through propeller redundancy and allows for more

controllability. DEP provides a wider range of aircraft maneuverability because a flight control system can individually adjust the speed and, in some cases, the thrust vector of each propeller (Kim, et al., 2021). Multiple independent rotors reduce the risk of crashing if one or more propeller malfunctions. However, DEP entails greater design complexity because of the considerable number of locations and engine operating characteristics that are possible.

Nearly all eVTOL aircrafts use electric motors to spin propellers that accomplish both lift and cruise operations. Electric motors can

- more efficiently convert battery energy to produce thrust at a lower cost,
- be more easily distributed around the aircraft to increase controllability,
- be coupled more compactly with their own battery to provide redundancy and prevent a single point of failure,
- produce less noise, which is an important consideration for acceptance in urban settings.

The many degrees of freedom in selecting the number of propellers, blades per propeller, fan diameter, and rotation speed exacerbate the design complexity of eVTOL aircrafts. The interactions between the propeller airflow vortices and wake with the fuselage and wings directly affect the efficiency of the overall propulsion system in a complex manner that is difficult to characterize and compare among designs (Yan, Lou, Xie, Chen, & Zhang, 2021). Kim et al. (2021) found that the forces and moments generated by the propellers can deteriorate the longitudinal and directional stabilities of an eVTOL aircraft (Kim, et al., 2021). Piccinini et al. (2020) found that the aerodynamic interaction of rotors can result in a substantial loss of propulsive efficiency, depending on their configuration and alignment on the airframe (Piccinini, Tugnoli, & Zanotti, 2020).

Current trends suggest that manufacturers have been adopting winged eVTOL architectures because they are more efficient for long range mobility applications. Bacchini and Cestino (2019) examined a variety of eVTOL design concepts and confirmed that winged architectures best serve long-range missions (Bacchini & Cestino, 2019). Wilke (2020) found that the wing benefits both hovering and cruise modes because it acts as a stator to increase the rotor efficiency (Wilke, 2020).

Winged eVTOL aircraft designs have so far converged to two architecture types: vectored thrust and transitioned thrust (TT) (Sripad & Viswanathan, 2021). Designers achieve thrust vectoring by using either tilt rotor (TR), tilt wing (TW), or folding wing (FW) designs. TT architectures avoid the operational complexities and weight of tilting mechanisms by using one set of fixed rotors for lifting and another set for cruising.

TT designs are popular because they reduce the risk of tilting mechanism failure. On the other hand, TT architectures must carry idle rotors during cruise mode, thus adding useless weight and parasitic drag. Some manufacturers attempt to reduce the drag of idle rotors by either folding their propeller blades into the airflow or retracting them into the airframe. Bacchini et al. (2021) found that retracting the propellers can reduce parasitic drag by 38% to yield a 13% increase in range, despite the added weight of the retraction system (Bacchini, Cestino, Magill, & Verstraete, 2021). Some TT designs also embed fixed rotors in the wings or fuselage to reduce drag, but any openings still create drag by disrupting laminar airflow.

TR designs are a popular approach to thrust vectoring. The ability to tilt each rotor independently provides more degrees of freedom for aircraft control in both hover and cruise modes. However, Pavel (2021) found that rotor pitch control requires more intelligence, including motor speed control, to minimize the effects of transient dynamics from the rotor-

motor coupling (Pavel, 2021). Relatively few designs use TW or FW architectures to achieve thrust vectoring. TW designs have the advantage of using all rotors for both lift and cruise modes while avoiding separate tilting mechanisms for individual rotors as well as eliminating the possibility of TR propeller downwash onto the wings during lifting operations. However, the tilting or folding operation from vertical lift to horizontal cruise takes time to reach the altitude and airspeed where the wings can provide adequate lifting forces. TW operation also requires trajectory optimization to safely transition between takeoff and cruise operations, which is still an active area of research (Chauhan & Martins, 2020). For passenger comfort, the extra time required to gradually transition between lifting and cruising consumes a significant amount of energy. For instance, in the analysis of a proposed TW aircraft design, Palaia et al. (2021) calculated that the transition from hover to cruise consumed approximately 8% of the available battery energy (Palaia, Salem, Cipolla, Binante, & Zanetti, 2021).

2.3 Flight Range Projections

Whereas the electrification of ground vehicles is rapidly approaching maturity, aircraft electrification is still just beginning (Bills, Sripad, Fredericks, Singh, & Viswanathan, 2020). Flight endurance is directly proportional to the energy density of a battery with a given weight constraint (Zong, Zhu, Hou, Yang, & Zhai, 2021). However, the range reported by some manufacturers may not necessarily include realistic operating considerations such as weather influences like headwinds and temperature or safety procedures that may require longer hover times (Hagag, Toepsch, Graf, Büddefeld, & Eduardo, 2021). Range may differ also based on the amount of energy kept as reserve to comply with regulations and safety guidelines (Kundu, Price, & Riordan, 2019).

A 2020 review of the literature on electric-propulsion aircraft found that the lithium ion (LI) battery chemistry was the most mature, with an energy density of 300 Wh/kg and approaching 450 Wh/kg by 2025 (Sahoo, Zhao, & Kyprianidis, 2020). Therefore, simply replacing the battery of existing aircraft designs without changing anything else will increase the average range by approximately 50% within five years. Beyond 2030, aircraft range can increase by more than 5-fold as other types of battery chemistries such as lithium-air reach 1750 Wh/kg.

Most eVTOL designs converge to a comparable size because aircraft weight increases with the cube of aircraft capacity before running into the limitations of available battery and charging station technologies (Warren, Garbo, Herniczek, Hamilton, & German, 2019). Lee et al. (2020) found that the MTOW has a direct effect on aircraft performance in terms of range, cruise speed, and stall speed (Lee, Tullu, & Hwang, 2020). Akash et al. (2022) presented the design of a TR eVTOL aircraft that they expect to carry 500-kilograms of payload for 500 kilometers by assuming the use of a 600 Wh/kg lithium-sulphur battery (Akash, et al., 2022). Their mission profile estimated that cruising at 200 km/h will account for 81% of the total energy use.

At the time of this literature review, there are no works relating to the development of a performance index that can help with an objective comparison of eVTOL designs.

3 Method

All winged eVTOL aircrafts must accomplish stable lift control to climb and land vertically precisely and safely. All winged aircrafts must reach a specified altitude to maintain the design cruise speed. The air density at different altitudes affects the cruise speed design choice. For mobility missions, cruising will dominate the flight time. Hence, the design of the PEX accounts only for the longitudinal flight distance traversed in cruise mode, and not the lifting operation. The next section derives the theoretical propulsive efficiency factor of a winged aircraft in cruise

mode to inform the definition of the proposed PEX. Figure 1 illustrates the overall workflow described in the subsections that follow.

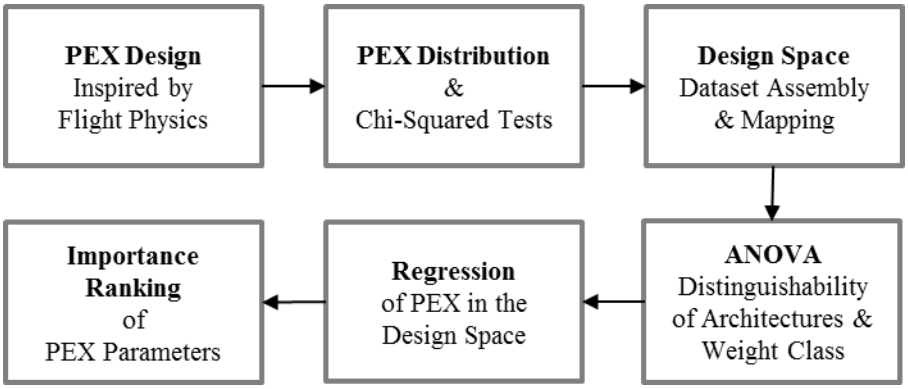

Figure 1: Workflow of the methods.

3.1 Flight Physics Review

The four forces acting on a winged aircraft as it pierces the air (fluid) are drag, thrust, lift, and weight (MIT, 1997). The propulsion system of an aircraft maintains its cruise speed by creating a steady thrust (horizontal force) to overcome the drag. Given a velocity, the resulting airflow creates lifting forces when the air density under the wings and other lifting surfaces of the airframe exceeds the air density above those surfaces. The wing cross section is an airfoil that forces the air to flow faster above it than below it. The Bernoulli principle states that

$$p + \frac{1}{2}\rho v^2 = c \tag{1}$$

where p is the pressure (force per unit area) that the air flow exerts on the airframe, ρ is the density of the air, v is the velocity of the airframe relative to the air, and c is a constant. The expression $\rho v^2/2$ is the dynamic pressure because it is a function of the velocity. An *increase* in velocity leads to a *decrease* in pressure because the total pressure must sum to a constant. For instance, fluid flowing through a narrow pipe section flows faster to keep the input and output flows constant.

By the flow continuity principle,

$$\rho \times A \times v = c \tag{2}$$

where *A* is the surface area. The design of an airfoil is such that the surface area on top is greater than that of the bottom. To understand the principle more easily, imagine an airfoil placed in the center of a pipe. The larger surface area on top of the airfoil results in more narrowing of the pipe than at the bottom. Therefore, the flow area on top of the airfoil decreases more than the flow area on the bottom. Given the same fluid density, the flow velocity *v* must *increase* in direct proportion to the area reduction. Per the Bernoulli principle, when *v* increases, the pressure must *decrease* to maintain the constant. Therefore, the pressure above the airfoil must be proportionally lower than the pressure below the airfoil. This pressure difference produces a net upward pressure that creates lift *L* in force units as

$$L = C_L \times \frac{1}{2}\rho v^2 \times S_L \tag{3}$$

where S_L is the lift surface area and C_L is a lift coefficient.

The lift generated is the perpendicular component of the vector sum of all the forces that the air exerts on the airframe while flowing around it. The C_L factor scales the dynamic pressure to create the lifting force, but it has been difficult to calculate (Akash, et al., 2022). Therefore, engineers estimate C_L by measuring the dependent factors. For example, designers can determine C_L via equation (3) by measuring S_L through volumetric change experiments and measuring *L* in a wind tunnel as a function of airflow speed. The lift must be equal to the aircraft weight to maintain its altitude at the desired cruise speed. Tilting the wing will also create lift by forcing airflow downwards, but a tilted wing also increases drag, which requires more thrust to maintain speed.

Drag is the resistance to airflow that the airframe experiences when moving through air. Drag is comprised of the air pressure in front of the airframe and friction from air moving along the body. The drag D is directly proportional to the dynamic pressure and the area A_D onto which the force acts as

$$D = C_D \times \frac{1}{2}\rho v^2 \times A_D \tag{4}$$

The lift must equal the maximum takeoff weight (MTOW) W_m of the aircraft such that

$$L = W_m = C_L \times \frac{1}{2}\rho v^2 \times S_L \tag{5}$$

Solving for the dynamic pressure yields

$$\frac{1}{2}\rho v^2 = \frac{W_m}{S_L C_L} \tag{6}$$

To maintain a cruise speed v, the propulsion system must continuously accelerate a mass of air to create a horizontal thrust force F_T that overcomes the drag such that

$$F_T = D = C_D \times \frac{1}{2}\rho v^2 \times A_D \tag{7}$$

Substituting the dynamic pressure yields

$$F_T = \frac{C_D}{C_L} \times \frac{A_D}{S_L} \times W_m \tag{8}$$

Engineers define the aerodynamic efficiency η_a of an airframe as the lift-to-drag ratio

$$\eta_a = \frac{C_L}{C_D}. \tag{9}$$

Hence

$$F_T = \frac{1}{\eta_a} \times \frac{A_D}{S_L} \times W_m \tag{10}$$

From fundamental physics, work is the product of force and distance and power is the work done per unit of time T. That is,

$$P = \frac{F_T \times D}{T} = F_T \times \frac{D}{T} = F_T \times v \tag{11}$$

Substituting equation (10) into equation (11) yields

$$P = \frac{1}{\eta_a} \times \frac{A_D}{S_L} \times W_m \times v \tag{12}$$

The propulsive efficiency factor of the aircraft is then

$$\eta_a = \frac{1}{P} \times \frac{A_D}{S_L} \times W_m \times v \tag{13}$$

The power needed from the battery is

$$P = \eta_b \times W_b \times \frac{1}{T} \tag{14}$$

where η_b is the energy density of the battery in Wh/kg, W_b is the weight of the battery in kilograms, and T is the flight endurance in hours. Substituting equation (14) into equation (13) yields

$$\eta_a = \frac{T}{\eta_b \times W_b} \times \frac{A_D}{S_L} \times W_m \times v \tag{15}$$

Rearranging and grouping terms yields

$$\eta_a = \frac{1}{\eta_b} \times \frac{A_D}{S_L} \times \frac{W_m}{W_b} \times T \times v \tag{16}$$

Rewriting equation (16) to verify that the unit of R is in distance yields

$$R = \eta_a \frac{S_L}{A_D} (\eta_b W_b) \frac{1}{W_m} \tag{17}$$

or

$$R = \eta_a \frac{S_L}{A_D} \frac{1}{Mg} J \tag{18}$$

which replaces $(\eta_b W_b)$ with J as the energy capacity of the battery in joules. The propulsive efficiency factor η_a and the lift-to-drag ratio S_L/A_D are unitless. The gross aircraft weight is in

Newton force units where $W_m = M \times g$ is the product of the maximum takeoff mass (kilograms) and the average acceleration $g = 9.81\ m \cdot s^{-2}$ on the earth's surface. Given that J is equivalent to the work unit of Newton-meter, R must be in the distance unit of meters.

The maximum takeoff weight (W_m) is the sum of the aircraft weight without fuel (W_a), the weight of the fuel (W_b), which is the battery for eVTOL aircrafts, and the weight of the payload (W_p). That is, $W_m = W_a + W_b + W_p$. Most manufacturers tradeoff battery weight for payload capacity, depending on the endurance needed for a mission. With battery weight being some proportion of the payload where $W_b = \gamma W_p$,

$$\eta_a = \frac{1}{\eta_b} \times \frac{A_D}{S_L} \times T \times v \times \frac{W_m}{\gamma W_p} \tag{19}$$

The payload ratio η_W is the ratio of the payload weight to the MTOW where

$$\eta_W = \frac{W_p}{W_m} \tag{20}$$

Hence,

$$\eta_a = \frac{1}{\eta_b \times \gamma} \times \frac{A_D}{S_L} \times \frac{1}{\eta_W} \times T \times v \tag{21}$$

Given that the cruise range R is the product of cruise speed v and endurance T, the propulsive efficiency factor simplifies to

$$\eta_a = \frac{1}{\eta_b \times \gamma} \times \frac{A_D}{S_L} \times \frac{1}{\eta_W} \times R \tag{22}$$

Figure 2 provides an additional perspective of the derived formulas by illustrating the interdependencies of each parameter and the final impact on flight endurance. The gray-shaded boxes indicate the independently controllable parameters based on key design goals and the unshaded boxes are the dependent parameters. Given the airframe material selected, such as carbon fiber composite, the MTOW will be directly proportional to the airframe volume, payload

capacity, weight of other equipment and materials such as the control hardware, wire harnesses, and motors, and the weight of the batteries.

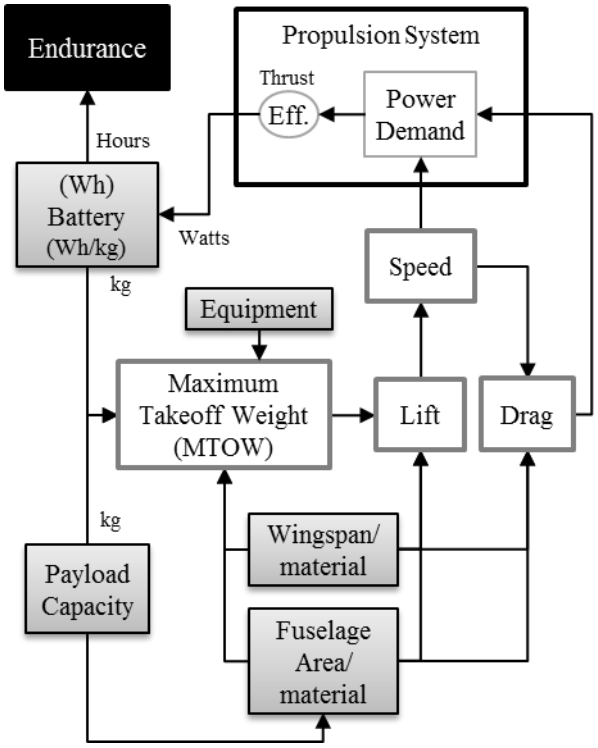

Figure 2: Interaction of aircraft design parameters.

The wing and some other portions of the aircraft body, such as the fuselage, produce both lift and drag forces. However, the wing dominates the amount of lift generated whereas the rest of the aircraft body dominates the drag contributions. Per equation (7), given the airframe aerodynamics, the amount of drag force produced depends on both the size of the drag surface area and the aircraft speed. Furthermore, per equation (5), the lift required to overcome the MTOW is a function of the aircraft speed. The propulsion system can produce the thrust required to overcome the drag and maintain the required speed by consuming the amount of power given by equation (11). The efficiency of the propulsion system modulates the actual amount of power demanded from the battery. Finally, the flight endurance (hours) depends on the amount of

energy stored in the battery (Watt-hour) and the rate that the propulsion system consumes it (Watts).

The formula for propulsive efficiency factor given by equation (22) indicates the change in propulsive efficiency needed to accommodate a change in any of the parameters while keeping the others constant. The following are a few examples:

1. Accommodating a larger drag area without changing anything else requires more efficiency.
2. The availability of a higher energy density battery for the same airframe (drag and surface area unchanged) will require proportionally less propulsive efficiency to maintain the same speed and endurance.
3. Achieving a lower MTOW without changing the payload capacity, for example by using lighter airframe materials and engines, increases η_W, which reduces the required propulsive efficiency.

3.2 Propulsion Efficiency Index

The derived propulsive efficiency factor η_a of equation (22) informs the definition of the proposed PEX. The main factors of η_a are the energy density of the battery η_b, the lift-to-drag surface area S_L/A_D, the payload ratio W_p/W_m, and the range R. The goal is to define a PEX that incorporates these key parameters in a manner that reflects a preferred performance level. That is, given equal values for the other parameters, the better performing design will have a higher value for the considered parameter, thus yielding a higher PEX value. In principle, all designs have access to the same energy density battery technology, so the PEX drops it from consideration as a parameter preference. Furthermore, when treating both the MTOW and range as independent parameter choices, the MTOW already includes the battery weight and the

endurance or range is proportional to the energy capacity of the battery. This means that the better performing design will have higher values for range R, payload ratio W_p/W_m, and drag-to-lift surface area A_D/S_L.

The choice of higher values for the range and payload ratio as better performance specifications is obvious, but the choice of a higher drag-to-lift surface area requires further explanation. That is, given two designs with the same range and payload ratio, one would prefer a smaller lift surface area than the drag surface area because wings that are longer than the length of an aircraft would be less space efficient for parking. Furthermore, a longer aircraft body, which the fuselage typically dominates, can accommodate more payload, and fit better in the existing rectangular parking spaces or terminal gates.

Aircraft providers often specify the range, endurance, speed, MTOW, payload capacity, and the maximum dimensions of the aircraft footprint. Manufacturers seldom disclose the lift-to-drag surface area S_L/A_D because it is usually part of their design trade secret. Without general access to the S_L/A_D value, the PEX instead utilizes the ratio of the airframe length, L, to the airframe width, W. That is, the L/W ratio becomes a proxy for the S_L/A_D ratio. The rationale is that the wingspan, which typically dominates the width footprint of an aircraft, provides the dominant portion of the lifting force. Similarly, the longitudinal members of an airframe, which the fuselage often dominates, account for most of the surface area that is subject to the frictional air flow that creates drag. The L/W ratio is the aspect ratio AR of the aircraft footprint.

All eVTOL aircrafts must climb to a specified altitude A before they can maintain the designed cruise speed. Higher altitudes have lower air density, which enables the aircraft to cruise faster or use less power to maintain the same cruise speed. However, it takes longer and thus requires more energy to reach a higher altitude. To account for variations in the design

cruise altitude, the PEX normalizes the horizontal flight range *R* by the vertical design altitude *A*. Hence, the proposed PEX is

$$\eta_{PEX} = \frac{L}{W} \times \frac{W_p}{W_m} \times \frac{R}{A} \tag{23}$$

which is unitless. This result answers the first research question posed in the introduction about the minimum set of independent parameters that could define a PEX.

3.3 Dataset Assembly

A few hundred manufacturers are currently developing drones to address the emerging markets for AAM. Table 1 summarizes the main winged aircraft architectures types along with their advantages and disadvantages. The constructed dataset includes published performance data from the websites or public records such as the patents or investor presentations from manufacturers announced before the end of the year 2021. The concatenation of Table 3 and Table 4 shows the data from 45 manufacturers that published all the data required to compute a PEX. Table 2 describes the variables in the constructed dataset.

As of the end of 2021, none of the designs were in commercial service. Hence, the values reported are either measurements from full-scale prototypes, projected from sub-scale prototypes, or proposed based on conceptual designs or simulations. For instances where the manufacturer did not disclose airframe dimensions, the author estimated the AR from top-down views available on the manufacturer's website, promotional videos, or patents. The cruise altitude is not available for all entries of the dataset. Therefore, all the PEX values use 10,000 feet (1.89 miles or 3048 meters), which is the typical altitude that helicopters fly for optimum control and to minimize the onset of hypoxia (Davis, Stepanak, Fogarty, & Blue, 2021). For those instances where the payload capacity is specified only as the number of passengers and

pilots, the entry uses the typical commercial airline estimate of 200 pounds per person plus 50 pounds for each passenger's luggage, excluding luggage for the pilots.

Table 1: Winged VTOL Architecture Types

Type	Advantages	Disadvantages
Tilt Rotor (TR). At least one set of rotors tilt to operate in both lifting and cruising modes.	Rotors are not idle in any mode—idle rotors are useless weight and may add drag unless enclosed. All rotors are available to maximize control and redundancy.	Weight, complexity, and possible failure of tilting mechanisms. Any propeller downwash onto the wings decreases lift efficiency. Transition from lift to cruise takes longer without separate cruise propellers.
Tilt Wing (TW). At least one portion of the wing, with fixed rotors attached, tilts to achieve both lifting and cruising modes.	Rotors are not idle during cruise. Avoids tilting individual rotors for fewer mechanisms. All rotors are available to maximize control and redundancy. Avoids downwash.	Weight, complexity, and possible failure of tilting mechanisms. Transition from lift to cruise takes longer without separate cruise propellers. More susceptible to wind gusts while hovering. Placing batteries in the wing requires a sturdier tilt mechanism.
Transitioned Thrust (TT). Fixed lift rotors become idle after transitioning to separate rotors for cruising.	Eliminates the weight, complexity, and possible failure of tilting mechanisms. Eliminates flight control complexity for rotor angle control and maintaining stability during tilting.	Exposed rotors can add to the drag. Rotor retraction or blade folding mechanisms can reduce drag but add weight and flight control complexity.
Folding Wing (FW). At least one portion of the wing, with fixed rotors attached, folds to operate in both lifting and cruising modes.	Needs less ground footprint. No idle rotors in any mode. Accommodating more rotors on the folding members increase controllability.	Weight, complexity, and possible failure of folding mechanisms.
Fixed Rotor (FR). Fixed position rotors adjust their relative speed to provide both lift and cruise operations.	Rotors are not idle in any mode. No tilting or folding mechanisms to increase weight or failure risk.	The airframe tilts up during vertical lift, which may cause discomfort if the cabin is not gimballed.

Table 2: Description of the Data Table Headers

Parameters	Description	Units or category
Company	Manufacturer of aircraft	unitless
Model	Aircraft model	unitless
TY	Type of eVTOL architecture	TR (tilt rotor), TT (transitioned thrust), TW (tilt wing), folding wing (FW), fixed rotor (FR)
W	Width of aircraft	meters
L	Length of aircraft	meters
AR	Aspect ratio of length to width	None
MTW	Maximum takeoff weight	kilograms
P	Payload (people or cargo)	kilograms
R	Distance traveled at cruise speed	kilometers
C	Cruise speed	kilometers-per-hour (KPH)
T	Time spent in cruise mode	minutes
PEX	Propulsive Efficiency Index	unitless

Table 3: eVTOL Data (Part I)

Company	Model	TY	W	L	AR	MTW	P	R	C	T	PEX	Data Source
ACS Aviation	Z-300	TW	8.0	7.1	0.89	1000.0	180.0	300.0	222.2	90.0	15.7	(ACS Aviation, 2021)
AIR EV	AIR ONE	FR	-	-	0.68	1170.0	200.0	177.0	160.9	60.0	6.8	(AIR EV, 2021)
Airbus	CityAirbus NG	TT	11.4	8.2	0.72	2200.0	453.5	80.0	120.0	40.0	3.9	(Airbus, 2021)
Archer	Maker	TR	12.2	9.3	0.76	2052.2	544.2	96.5	241.4	24.0	6.4	(Archer Aviation Inc., 2021)
Aurora Flight Sciences	Pegasus PAV	TT	8.5	9.1	1.07	798.2	224.9	80.5	180.2	26.8	8.0	(Aurora Flight Sciences, 2021)
Autoflight	V1500M	TT	12.8	10.3	0.80	1500.0	453.5	250.0	200.0	75.0	20.0	(Autoflight, 2021)
Autonomous Flight	Y6S	TR	6.1	6.7	1.10	907.0	226.8	128.7	201.1	38.4	11.6	(Autonomous Flight, 2021)
Autonomous Flight	Y6S plus	TR	-	-	0.94	2630.4	657.6	128.7	201.1	38.4	9.9	(Autonomous Flight, 2021)
Bartini Inc.	Bartini eVTOL	TR	5.5	5.5	1.00	1502.7	400.0	150.0	300.0	30.0	13.1	(Bartini, 2021)
Bell	APT 70	FR	2.7	1.8	0.67	165.0	45.0	56.3	160.9	21.0	3.4	(Bell, 2021)
Bell	Nexus 4EX	TR	12.9	10.1	0.78	3718.8	544.2	96.5	241.4	24.0	3.6	(Bell, 2021)
Beta Technologies	Alia-250	TT	15.2	10.9	0.71	3174.1	680.3	463.0	194.5	142.9	23.2	(BETA Technologies, 2021)
Braunwagner	SkyCab	TT	12.0	10.1	0.84	2999.1	362.8	100.0	240.0	25.0	3.3	(SkyCab, 2021)
Digi Robotics	Droxi UAD-M20	TR	2.2	1.6	0.74	19.5	5.0	150.0	100.0	90.0	9.4	(Sigler, 2018)
Dufour Aerospace	Aero3	TW	14.8	14.6	0.98	2799.5	749.7	120.7	350.0	20.7	10.4	(Dufour Aerospace, 2021)
EHang	VT-30	TT	12.5	6.8	0.54	881.2	181.4	300.0	180.0	100.0	11.0	(EHang Holdings Ltd., 2021)
eMagicAircraft	eMagic One	TT	7.7	7.2	0.94	400.0	145.1	144.0	144.0	60.0	16.1	(eMagic Aircraft, 2021)
Eve UAM	Eve	TT	11.0	13.0	1.18	1542.0	544.2	96.5	241.4	24.0	13.2	(Eve UAM, LLC, 2021)
Flyter	PAC 720-200	TT	7.0	6.3	0.89	720.0	200.0	160.0	250.0	38.4	13.0	(Flyter, 2021)
Grug Group	SBX	TR	10.3	7.6	0.74	2150.0	544.2	310.0	310.0	60.0	19.1	(Grug Group LLC, 2017)
Horyzn Aerospace	Silencio Gamma	TT	3.6	2.0	0.54	12.0	2.0	51.0	70.0	40.0	1.5	(HORYZN, 2021)
Hyundai UAM	S-A1	TR	15.0	0.0	0.64	3668.5	544.2	99.8	289.6	20.7	3.1	(Hyundai Motor Group, 2021)
Jaunt Air Mobility	Journey	TT	15.2	15.2	1.00	2721.1	544.2	144.8	281.6	30.9	9.5	(Jaunt Air Mobility LLC., 2021)
Joby Aviation	S4	TR	11.6	6.4	0.55	2176.9	544.2	241.4	265.5	54.5	10.9	(Joby Aviation, 2021)
KARI	OPPAV	TR	7.0	6.2	0.88	650.0	100.0	50.0	200.0	15.0	2.2	(KARI, 2021)
Kitty Hawk	Heaviside	TR	6.1	4.7	0.77	374.6	113.4	160.9	289.6	25.0	12.3	(Kittyhawk, 2021)
Leap Aeronautics	Leap XE6	TT	12.0	8.0	0.67	2180.0	500.0	200.0	250.0	48.0	10.0	(Leap Aeronautics, 2021)

Table 4: eVTOL Data (Part II)

Company	Model	TY	W	L	AR	MTW	P	R	C	T	PEX	Data Source
Lilium	Jet (7 seat)	TR	13.9	8.5	0.61	3174.6	771.0	249.4	281.6	53.1	12.2	(Lilium GMBH., 2021)
Micor Technologies	VAGEV	FW	6.1	5.1	0.83	600.0	200.0	80.0	130.0	36.9	7.2	(Micor Technologies, 2021)
Napoleon Aero	Napoleon Aero	TT	-	-	0.79	1500.0	400.0	100.0	241.4	24.9	6.9	(Izvestia News, 2017)
Opener	BlackFly V3	FR	4.1	4.1	0.99	246.3	90.7	40.2	99.8	24.2	4.8	(Opener, 2021)
Orca Aerospace	Orca	TR	-	-	0.68	1814.1	300.0	140.0	204.0	41.2	5.2	(Orca Aerosapce, 2021)
Overair (Karem)	Butterfly	TR	13.7	10.0	0.73	3628.1	498.9	160.9	201.1	48.0	5.3	(Overair, Inc., 2021)
PteroDynamics	Transwing	FW	3.8	2.0	0.54	26.2	6.8	247.8	101.4	147.0	11.3	(Ptero Dynamics, Inc., 2021)
Samad Aerospace	S5M Cargo	TR	8.0	6.7	0.84	600.0	60.0	217.2	152.9	85.3	6.0	(Samad Aerospace, 2021)
Skynet Project SRL	Genesys X-1	TR	6.0	3.5	0.58	139.7	49.9	99.8	180.2	33.2	6.8	(Giurca, 2021)
Terrafugia	TF-2A	TT	7.5	7.2	0.96	1200.0	200.0	100.0	180.0	33.3	5.2	(Terrafugia, 2021)
teTra Aviation	Mk-5	TT	8.6	6.2	0.71	567.0	78.9	75.6	108.0	42.0	2.5	(teTra Aviation Corp., 2021)
Vertical Aerospace	VA-X4	TR	14.9	13.1	0.88	2267.6	449.9	160.9	321.8	30.0	9.2	(Vertical Aerospace, 2021)
Volocopter	Voloconnect	TT	-	-	1.00	1596.4	399.1	100.0	180.0	33.3	8.2	(Nicola, 2021)
Voyzon Aerospace	e-VOTO	TR	8.0	4.3	0.53	726.8	226.8	125.0	250.0	30.0	6.8	(Voyzon Aerospace, 2021)
VTOL Aviation India	Abhiyaan_ENU800	TT	10.8	7.5	0.69	800.0	200.0	250.0	180.0	60.0	14.2	(VTOL Aviation India, 2021)
Wing (Alphabet)	Wing	TT	1.0	1.3	1.30	6.3	1.2	19.3	104.4	11.1	1.5	(Wing Aviation LLC., 2021)
Wingcopter	Wingcopter 198	TT	2.0	1.5	0.77	25.0	5.0	75.0	100.0	45.0	3.8	(Wingcopter, 2021)
Wisk	Cora	TT	11.0	6.4	0.58	1451.2	181.4	40.2	160.9	15.0	1.0	(Wisk Aero LLC., 2021)

3.4 Design Space

Figure 3 plots the payload capacity (kilograms) against the reported cruise range (kilometers) for the dataset described in the previous section.

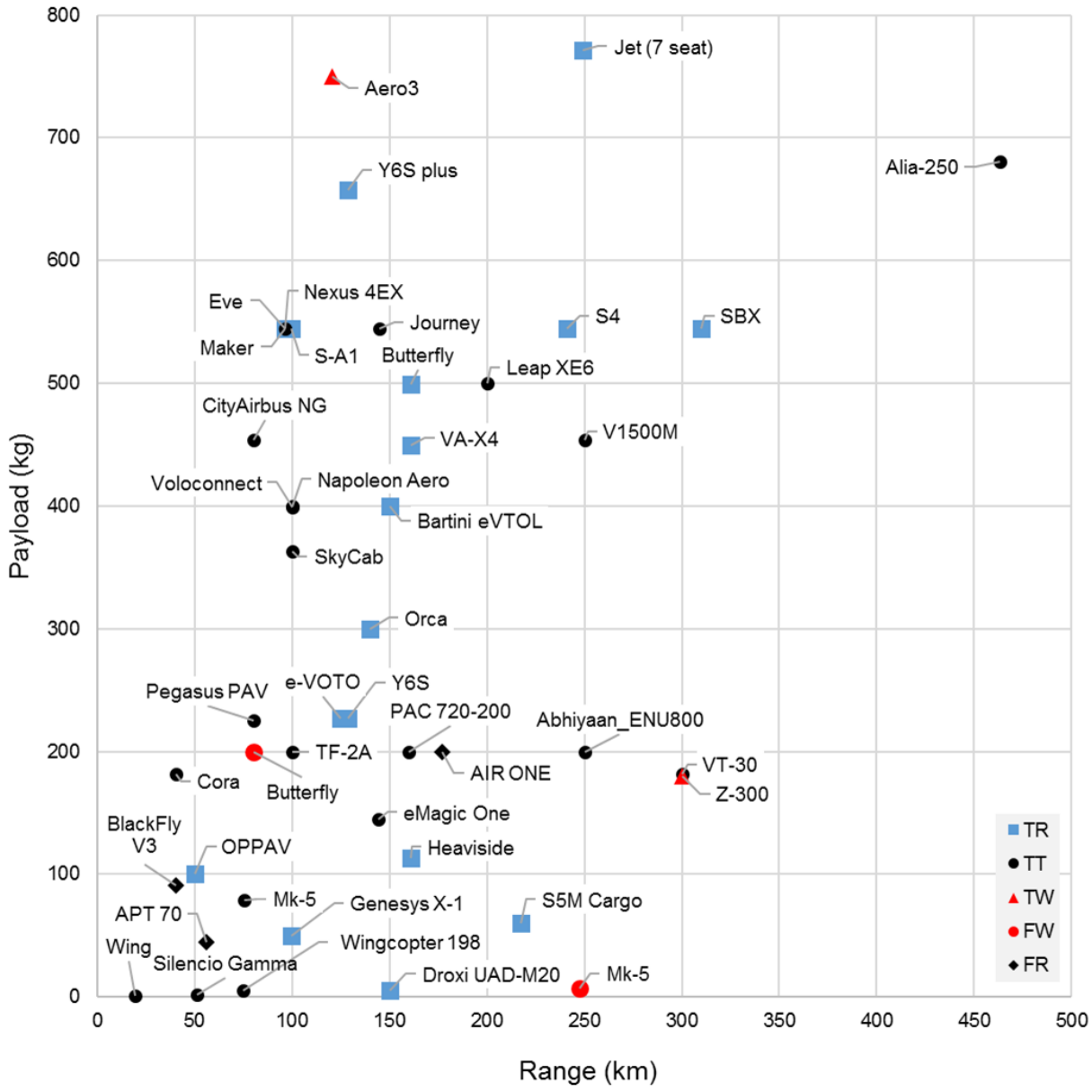

Figure 3: Aircraft model represented by the payload (kg) and range (km) reported.

The purpose of Figure 3 is to illustrate the spread of stated capabilities in the current design

space for each architecture type. The author cautions against making performance judgements based on this chart because those are the manufacturer's reported values. Also, at this snapshot in time, none of manufacturers deployed a certified design into commercial service.

4 Results and Discussion

The next subsections discuss the distributions of the PEX and its independent parameters, the associations between PEX and the mainstream architecture types, associations between the PEX and aircraft weight class, and the independent parameter importance ranking.

4.1 Design Parameter Distributions

This section answers the second research question posed in the introduction about the PEX distribution. Figure 4 plots the histogram (bars) and best fit distribution for the a) PEX, b) unnormalized range, cruise speed, payload ratio (PR) and aspect ratio (AR). The inset indicates the mean μ and standard deviation σ of each distribution.

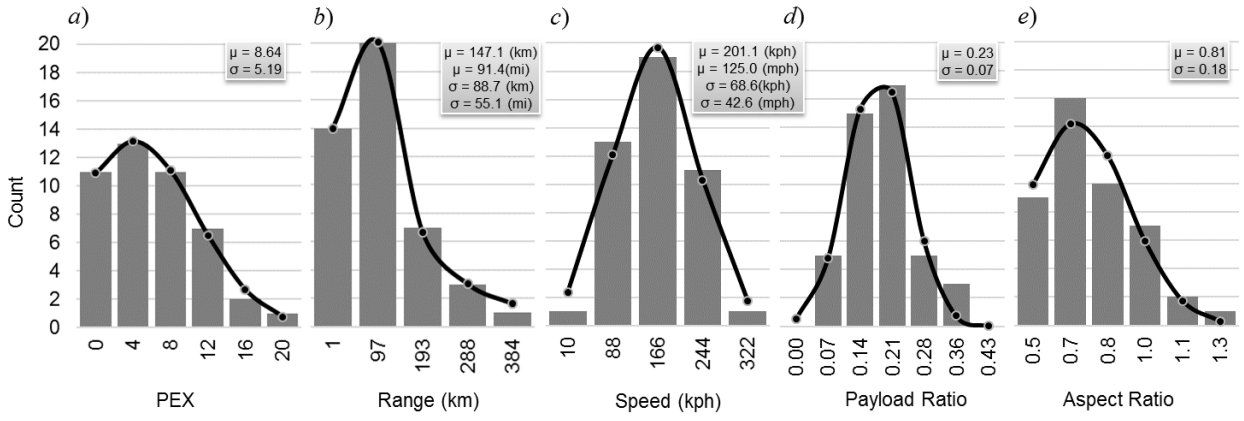

Figure 4: Distributions of a) PEX, b) Range, c) Speed, d) Payload Ratio, and e) Aspect Ratio

The solution to the following optimization problem provided the parameters for the best fit distribution:

$$\begin{aligned} &\underset{X_i}{\text{minimize}} \quad e = \sum_{i=1}^{B} (H_i - f_i)^2 \\ &\text{subject to} \quad \alpha > 0, \sigma > 0, \mu > 0 \text{ and } N \geq B \geq 4 \\ &\text{where} \quad f_i = \frac{\alpha}{\sqrt{2\pi\sigma^2}} e^{-\frac{(X_i-\mu)^2}{2\sigma^2}}, \; i = 1, 2, \ldots, B \end{aligned} \tag{24}$$

H_i are the counts for values within interval X_i of histogram bin i. The function f_i is the tested distribution. The optimization solved for the amplitude α, mean μ, and variance σ^2 combination of the function that minimized the sum-of-squares (SOS) error e, subject to the constraints indicated. The optimization procedure also adjusted the number of bins B within the constraint range to calculate the Pearson's chi-squared statistic

$$\chi_k^2 = \sum_{i=1}^{B} \frac{(H_i - D_i)^2}{D_i} \tag{25}$$

and to maximize the p-value associated with that statistic. The letter k represents the degrees-of-freedom (*df*) for the chi-squared statistic. The *df* was B minus the three estimated parameters α, μ, and σ, so the lower bound on the number of bins was 4 to ensure that the minimum *df* was at least unity. Hence, any minimum p-value that was less than 0.05 rejected the null hypothesis that the distribution followed the function tested (Agresti, 2018). Otherwise, the test could not reject the null hypothesis that the distribution followed the function tested.

Table 5 summarizes the statistics for each best fit distribution, null hypothesis H0 for the distribution type evaluated, the chi-squared statistic, the p-value, and the test result. All p-values were much larger than 0.05, therefore, none of the tests could not reject the null hypothesis for the functions of H0. The fitted function f_i was the lognormal for range and the normal or Gaussian for the other variables.

Table 5: Parameters of the Performance Variable Distributions and Chi-squared Tests.

Parameter	PEX	Range (km)	Speed (kph)	PR	AR
Mean	8.64	147.06	201.39	0.23	0.81
STD	5.19	88.66	68.66	0.07	0.18
Min	0.96	19.31	70.00	0.10	0.53
Max	23.25	462.99	350.00	0.37	1.30
CV	0.60	0.60	0.34	0.30	0.22
Skewness	0.74	1.33	0.07	0.13	0.56
Kurtosis	0.34	2.37	-0.69	-0.64	0.04
DOF	5	4	4	6	5
$\chi 2$ Statistic	0.28	0.25	1.25	7.20	2.50
$\chi 2$ p-value	0.99	0.99	0.87	0.31	0.77
H0	Normal	Lognormal	Normal	Normal	Normal
Reject H0	No	No	No	No	No

The mean values for range and speed were approximately 147 km (91 miles) and 201 kph (125 mph), respectively. The mean payload ratio accounted for nearly one-quarter of the MTOW. On average, aircrafts were wider than their length with a mean length-to-width aspect ratio of 0.81. The coefficient of variation CV measured the standard deviation proportion of the mean, which was also an indication of the relative spread of each variable. The results show that the spread of the unnormalized range was 1.8, 2.0 and 2.7 times that of the speed, PR, and AR, respectively. That is, there was a relatively larger spread in range than speed, PR, or AR in the design space. Consequently, the spread in PEX reflected the spread in range.

4.2 Architecture Distinguishability

This section answers the third research question posed in the introduction about any association between the PEX and the eVTOL architecture types. The box plot of Figure 5 compares the PEX distribution and fundamental statistics for each architecture type. The numbers above the blue box are the mean and standard deviation. The blue and yellow vertical lines indicate the locations of the mean and median values, respectively. The gray vertical lines intersect the horizontal axis to visualize how the means compare. The horizontal extent of the blue box and the associated numbers indicate values between the first (25%) and third (75%) quartiles. The dashed horizontal

line indicates the extent of those values from the minimum to the maximum. The values in the boxes on the right indicate the number of samples *N* evaluated.

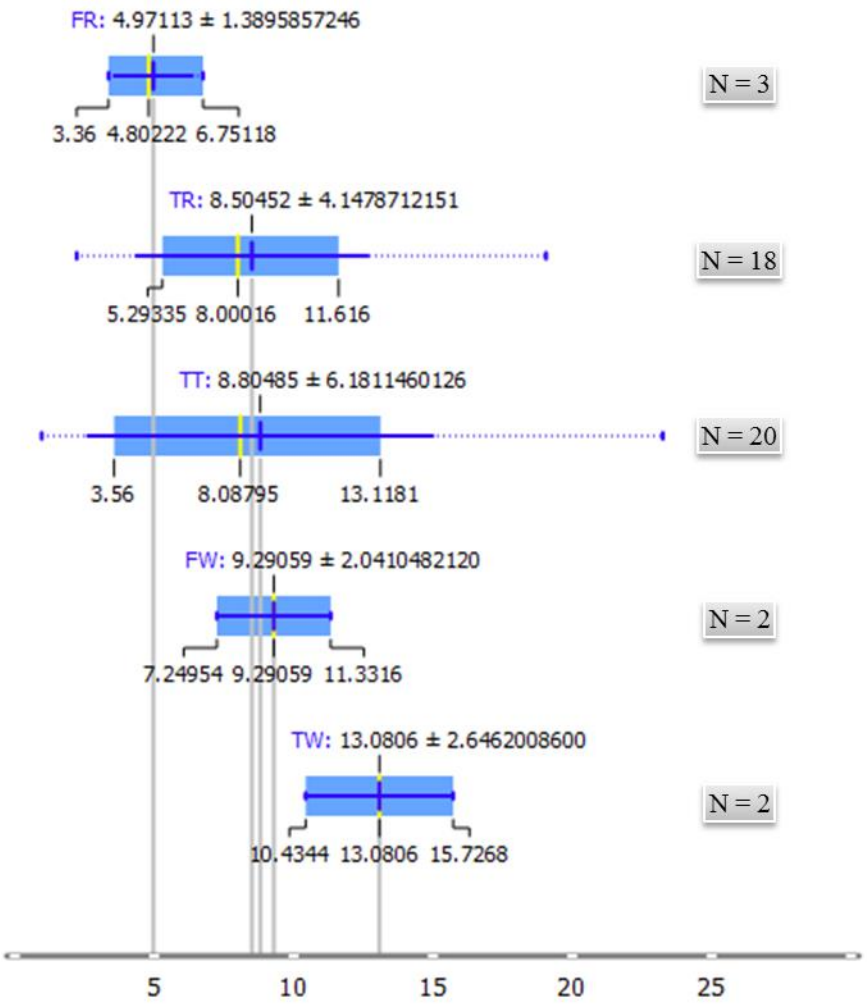

Figure 5: PEX distributions and ANOVA for the five drone architecture types.

Table 6 summarizes the results of an ANOVA test for the PEX, range, AR, and PR. The ANOVA test produced a statistic of 0.740 and a p-value of 0.570 for the PEX distribution. Therefore, the test could not reject the hypothesis that the PEX means are the same across all architecture types. The test resulted in the same conclusion for all variables. There were relatively few samples of the FR, FW, and TW. Hence, removing them resulted in a more

stringent Student's t-test on the remaining TR and TT samples. As shown in Figure 6, the t-test showed there was no significant difference between the PEX of those design based on a p-value of 0.860.

Table 6: ANOVA Tests Across All Architecture Types.

Parameter	ANOVA	p-value
PEX	0.740	0.570
Range	0.592	0.670
PR	0.706	0.593
AR	0.835	0.511

Conducting a separate ANOVA test on the few FR, FW, and TW samples suggest that there is a significant difference among their PEX based on a p-value of 0.067. However, the test is still inconclusive because of the relatively small number of samples.

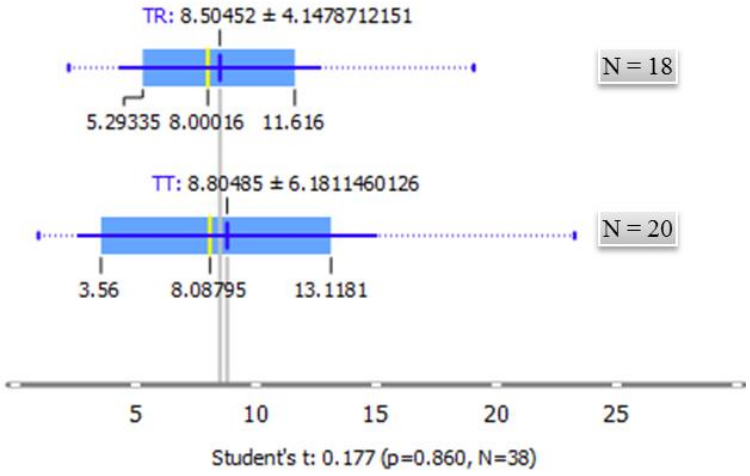

Figure 6: PEX distributions and t-test for the TR and TT drone architecture types.

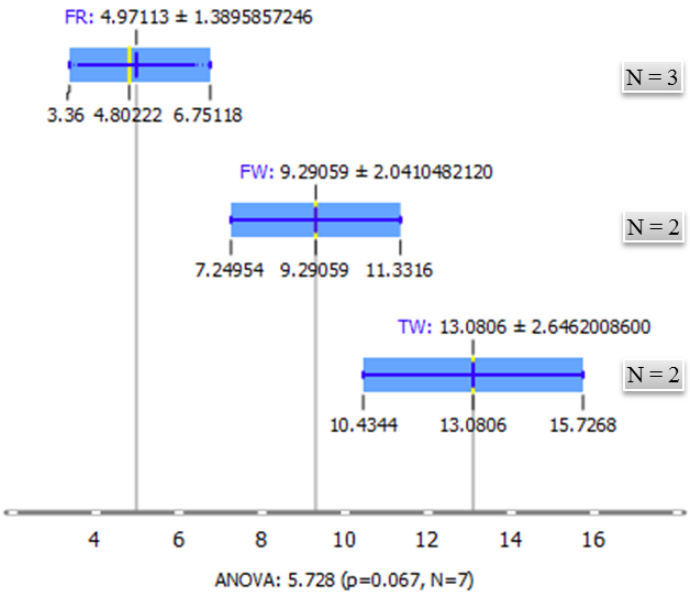

Figure 7: PEX distributions and ANOVA for the FR, FW, and TW drone architecture types.

4.3 PEX by Weight Class

The definition of the PEX is agnostic to the aircraft size or weight. However, per the fourth research question posed in the introduction, it is unclear if there is a statistical association between aircraft weight and PEX in the present design space. Derived using k-means clustering, the low weight class (CL) was up to 1,600 pounds, the medium weight class (CM) was between 1,600 and 4,800 pounds, and the high weight class (CH) was above 4,800 pounds. Figure 8 shows a box plot of the MTOW (pounds) by weight class. The ANOVA statistic (117.196) and p-value (0.000) shown rejects the null hypothesis that the distributions are the same. Therefore, the three weight classes are statistically different. The scatter plot of Figure 9 illustrates the co-distribution of PEX and MTOW by weight class. The scatter plot shows no clear association between the aircraft weight and the PEX. The R^2 value of the regression is 0.12.

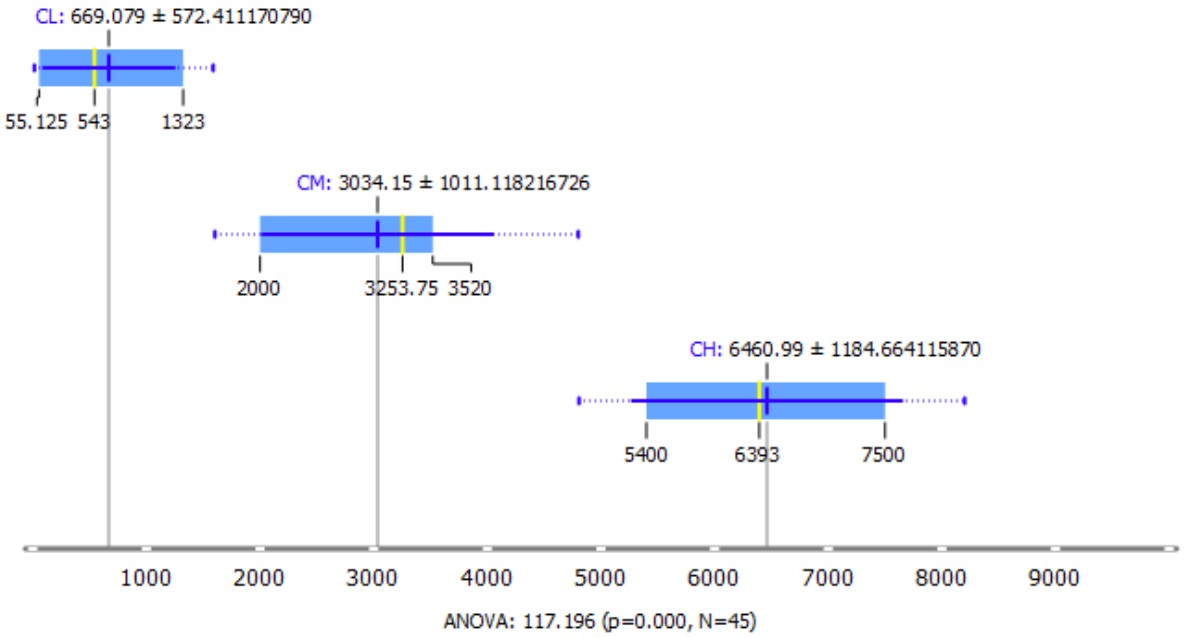

Figure 8: Box plot of MTOW (pounds) by weight class.

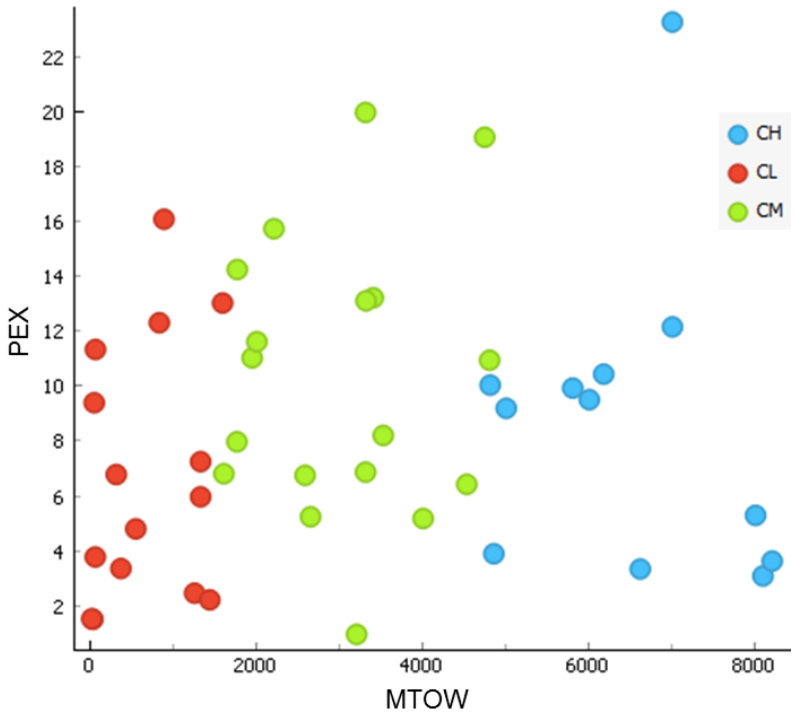

Figure 9: Scatter plot of PEX against MTOW by weight class.

Figure 10 shows a box plot of the PEX by weight class. Based on the ANOVA statistic (1.821) and the p-value (0.174), the statistical test cannot reject the null hypothesis that the PEX distributions are the same across the three weight classes. The conclusion, therefore, is that there is no association between the aircraft weight and the PEX.

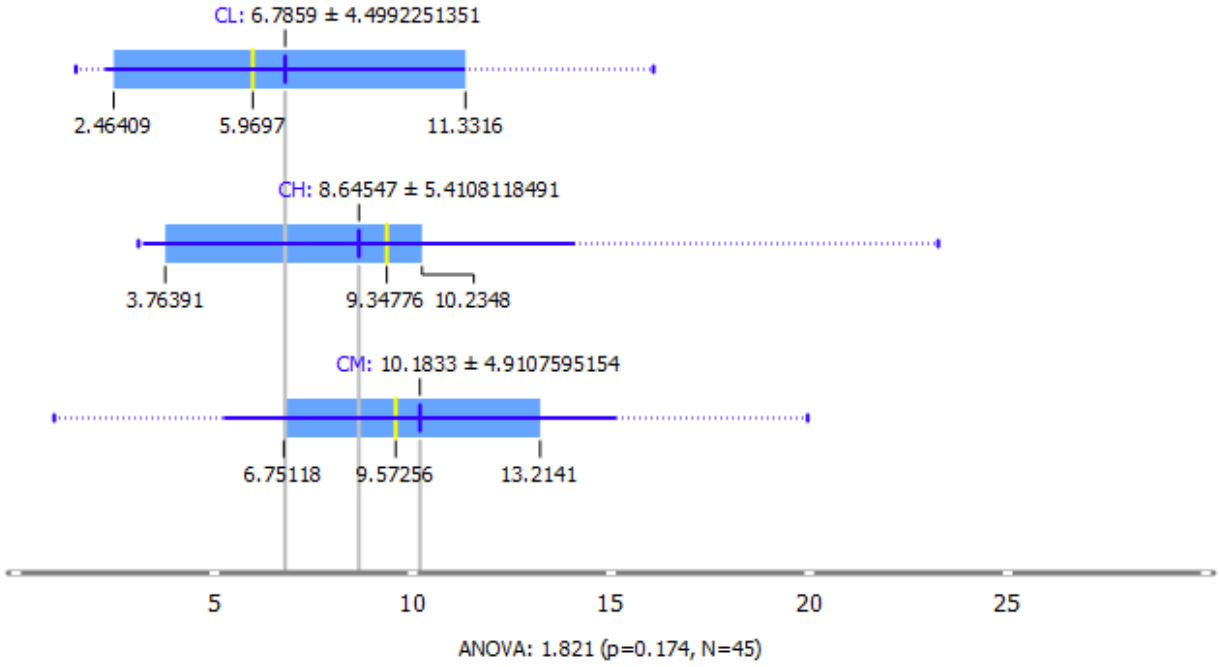

Figure 10: Box plot of PEX by weight class.

4.4 Ranking PEX Parameters

This section answers the fourth and fifth research questions posed in the introduction. The PEX is a product of three independent parameters, namely the altitude normalized range *RA*, the payload ratio *PR*, and the aspect ratio *AR*. A linear regression model can reveal the extent that those three variables explain the PEX distribution in the design space. The linear regression model is

$$\hat{y} = \alpha_3 \times AR + \alpha_2 \times PR + \alpha_1 \times RA + \alpha_0 \tag{26}$$

where the variable coefficients are $\{\alpha_1, \alpha_2, \alpha_3\}$ and α_0 is the regression constant. With

normalized variables, the relative weights of the coefficients for the fitted model are equivalent to the rank of their influence on the dependent variable.

Table 7 summarizes the regression outcome based on [0, 1] variable normalization, which kept all the variable coefficients positive. Table 7 also shows the weights for the unnormalized variables to demonstrate that without variable normalization, one could misinterpret the RA as being unimportant relative to PR and AR. The regression R^2 value was 0.919 and the standard error of the regression was 1.53 for either the normalized or unnormalized parameter values. The standard error of the regression indicated that on average, the PEX values were 1.53 units away from the regression line, which was significantly smaller (29.5%) than the PEX standard deviation. That is, the regression error was small relative to the PEX spread, which indicates a good fit.

The standard error (Std. Err.), t-statistic, and p-value columns are associated with the regression of the [0, 1] normalized variables. The standard error listed is the standard deviation in the prediction of each coefficient. The t-statistic is the size of the coefficient as a proportion of the standard error. The p-value, calculated from the t-statistic and the degrees-of-freedom in the data, is the probability that the coefficient is zero. All the p-values were much less than 0.05, which is the well-established threshold for statistical significance. Therefore, the p-value rejected the null hypothesis that any of the coefficients were zero.

Table 7: Parameters of the Regression Model.

Coefficients	**Unnormalized**	**[0, 1]**	**Std. Err.**	**t-statistic**	**p-value**
Constant	-12.20	-4.04	0.71	-5.68	10^{-5}
RA	0.08	23.09	1.21	19.05	10^{-5}
PR	29.86	8.01	0.91	8.85	10^{-5}
AR	7.84	6.02	1.04	5.79	10^{-5}

Per the classic interpretation of R^2, the linear model estimated from parameter variations in the design space explained 0.919 or approximately 92% of the PEX variations. In other words, approximately 92% of the PEX variation in the design space fitted the linear model. The R^2 value also provided that same level of confidence in the relative weights estimated for the design parameters. The results indicated that variations in the range had the most influence. The PR and AR variables had 35% and 26% less influence on the dependent variable than RA, respectively.

5 Conclusions

Advanced air mobility will embrace new modes of transport based on emerging eVTOL aircrafts. At the time of this analysis, there were no eVTOL aircraft operating commercial services. The current design space for eVTOL aircrafts is complex. Manufacturers have been transitioning from wingless to winged architectures because they are more energy efficient for long distance operations. Five fundamental winged architecture types have emerged: transitioned thrust (TT), tilt rotor (TR) vectored thrust, tilt wing (TW) vectored thrust, folding wing (FW) vectored thrust, and fixed rotor (FR). Potential adopters and service providers currently have no means to objectively compare designs along a performance spectrum.

Using the fundamentals of flight physics, this work defined a propulsion efficiency index (PEX) as a planning tool to compare the performance of existing and emerging eVTOL designs. The only specifications needed are the range, payload ratio, and aspect ratio, all of which are commonly available to the public. A histogram-optimization procedure revealed that the PEX distribution in the design space of 45 manufacturers is lognormal. The distributions of the independent parameters are lognormal for range, and normal for both the payload ratio and aspect ratio. The application of ANOVA revealed that there was no association between the PEX and the main eVTOL architecture types nor the aircraft weight. A multilinear regression showed

that the three dependent parameters of the PEX explained more than 90% of the PEX distribution in the present design space. The ranking of parameter explanation from highest to lowest weight was range, payload ratio, and aspect ratio. Planners can use the PEX to forecast future performance based on anticipated improvements in the energy density of batteries and the reduced weight of new airframe materials. Future work will update the dataset with performance specification based on commercially deployed services to compare the PEX distribution with the current distribution.

6 References

ACS Aviation. (2021). *Product Specifications*. Retrieved 12 24, 2021, from https://www.acs-solutions.com.br/index.php/produtos

Agresti, A. (2018). *Statistical Methods for the Social Sciences* (5th ed.). Boston, Massachusetts, U.S.: Pearson.

AIR EV. (2021). *Pushing the Envelope of Electric Aviation*. Retrieved 12 24, 2021, from https://www.airev.aero/

Airbus. (2021). *CityAirbus NextGen*. Retrieved 12 24, 2021, from https://www.airbus.com/en/innovation/zero-emission/urban-air-mobility/cityairbus-nextgen

Akash, A., Raj, V. S., Sushmitha, R., Prateek, B., Aditya, S., & Sreehari, V. M. (2022). Design and Analysis of VTOL Operated Intercity Electrical Vehicle for Urban Air Mobility. *Electronics, 11*(1), 20. doi:10.3390/electronics11010020

Archer Aviation Inc. (2021). *Introducing Maker*. Retrieved 12 24, 2021, from https://www.archer.com/maker

Aurora Flight Sciences. (2021). *Urban Air Mobility*. Retrieved 12 24, 2021, from https://www.aurora.aero/urban-air-mobility/

Autoflight. (2021). *Products*. Retrieved 12 24, 2021, from https://www.autoflight.com/en/products/

Autonomous Flight. (2021). *Introducing the Revolutionary Y6S Plus - Six Seater Electric VTOL Aircraft*. Retrieved 12 24, 2021, from https://autonomousflight.com/

Ayamga, M., Akaba, S., & Nyaaba, A. (2021). Multifaceted applicability of drones: A review. *Technological Forecasting and Social Change, 167*. doi:10.1016/j.techfore.2021.120677

Bacchini, A., & Cestino, E. (2019). Electric VTOL Configurations Comparison. *Aerospace, 6*(3), 26. doi:10.3390/AEROSPACE6030026

Bacchini, A., Cestino, E., Magill, B., & Verstraete, D. (2021). Impact of lift propeller drag on the performance of eVTOL lift+cruise aircraft. *Aerospace Science and Technology, 109*, 106429. doi:10.1016/j.ast.2020.106429

Bartini. (2021). *The Future of Air Travel*. Retrieved 12 24, 2021, from https://www.bartini.aero/#product

Baur, S., Schickram, S., Homulenko, A., Martinez, N., & Dyskin, A. (2018). *Urban Air Mobility: The rise of a new mode of transportation.* Munich: Roland Berger GmbH. Retrieved from https://www.rolandberger.com/publications/publication_pdf/Roland_Berger_Urban_Air_Mobility.pdf

BBC Research. (2020). *Drone Technology and Global Markets.* Wellesley, Massachusetts: Business Communications Company (BCC) Inc. Retrieved from https://www.bccresearch.com/market-research/instrumentation-and-sensors/drone-technology-global-markets.html

Bell. (2021). *Bell APT*. Retrieved 12 24, 2021, from https://www.bellflight.com/products/bell-apt

Bell. (2021). *Bell Nexus*. Retrieved 12 24, 2021, from https://www.bellflight.com/products/bell-nexus

BETA Technologies. (2021). *ALIA-250c*. Retrieved 12 24, 2021, from https://www.beta.team/aircraft/

Bills, A., Sripad, S., Fredericks, W., Singh, M., & Viswanathan, V. (2020). Performance Metrics Required of Next-Generation Batteries to Electrify Commercial Aircraft. *ACS Energy Letters*. doi:10.1021/acsenergylett.9b02574

Brandessence. (2021). *Drones Market By Type (Commercial Drones, Fixed-Wing Drones, VTOL Drones, Nano Drones And Others), By Application (Law Enforcement, Precision Agriculture, Media And Entertainment, Surveying And Mapping And Others), Industry Analysis, Trends, And Forecast.* London: Brandessence Market Research and Consulting Pvt Ltd. Retrieved from https://brandessenceresearch.com/technology-media/global-drone-market-2018-2024

Chauhan, S., & Martins, J. (2020). Tilt-Wing eVTOL Takeoff Trajectory Optimization. *Journal of Aircraft, 57*(1), 93-112. doi:10.2514/1.C035476

Cohen, A., Shaheen, S., & Farrar, E. (2021). Urban Air Mobility: History, Ecosystem, Market Potential, and Challenges. *IEEE Transactions on Intelligent Transportation Systems, 22*(9). doi:10.1109/TITS.2021.3082767

Constantine, D. (2020). *The Future of the Drone Economy.* Levitte Capital LLC. Retrieved from https://levitatecap.com/levitate/wp-content/uploads/2020/12/Levitate-Capital-White-Paper.pdf

Davis, J., Stepanak, J., Fogarty, J., & Blue, R. (2021). *Fundamentals of Aerospace Medicine.* (J. Davis, Ed.) Wolters Kluwer Health.

Dufour Aerospace. (2021). *Aero3 - Welcome to Versatile and Efficient VTOL*. Retrieved 12 24, 2021, from https://www.dufour.aero/aero3

EHang Holdings Ltd. (2021). *EHang Long-Range VT-30 AAV Makes Global Debut Before Zhuhai Airshow*. Retrieved 12 24, 2021, from https://ir.ehang.com/news-releases/news-release-details/ehang-long-range-vt-30-aav-makes-global-debut-zhuhai-airshow

eMagic Aircraft. (2021). *eMagic One – An eVTOL that really works*. Retrieved 12 24, 2021, from https://emagic-aircraft.com/#details

Eve UAM, LLC. (2021). *Eve Rio Experience*. Retrieved 12 24, 2021, from https://eveairmobility.com/rio-experience/

FAA. (2020). *National Plan of Integrated Airport Systems (NPIAS) 2021-2025.* Washington, DC: Federal Aviation Administration (FAA). Retrieved from https://www.faa.gov/airports/planning_capacity/npias/

FCAB. (2021). *National Blueprint for Lithium Batteries: 2021-2030.* Washington DC: Federal Consortium for Advanced Batteries. Retrieved from https://www.energy.gov/eere/vehicles/articles/national-blueprint-lithium-batteries

Flyter. (2021). *Flyter Products*. Retrieved 12 24, 2021, from https://flyter.aero/en/products

Garrow, L., German, B., & Leonard, C. (2021). Urban air mobility: A comprehensive review and comparative analysis with autonomous and electric ground transportation for informing future research. *Transportation Research Part C-emerging Technologies, 132*, 103377. doi:10.1016/J.TRC.2021.103377

Giurca, L. (2021, November 9). Cost Effective Ultra-Efficient VTOL Aircraft Genesys X-2. Retrieved from https://www.linkedin.com/pulse/cost-effective-ultra-efficient-vtol-aircraft-genesys-x-2-liviu-giurca/

Grug Group LLC. (2017). *Grug Group Future Technologies*. Retrieved 12 24, 2021, from https://www.gruggroup.com/copy-of-charter-flights-2

Guo, Y., Souders, D., Labi, S., Peeta, S., Benedyk, I., & Li, Y. (2021). Paving the way for autonomous Vehicles: Understanding autonomous vehicle adoption and vehicle fuel choice under user heterogeneity. *Transportation Research Part A: Policy and Practice, 154*(2021), 364-398. doi:10.1016/j.tra.2021.10.018

Hagag, N., Toepsch, F., Graf, S., Büddefeld, M., & Eduardo, H. (2021). *Maximum total range of eVTOL under consideration of realistic operational scenarios.* Retrieved from https://evtol.news/aircraft

HORYZN. (2021). *Project Silencio*. Retrieved 12 24, 2021, from https://horyzn.org/silencio/

Hyundai Motor Group. (2021). *Supernal Urban Air Mobility*. Retrieved 12 24, 2021, from https://supernal.aero/

IEA. (2021). *The Role of Critical Minerals in Clean Energy Transitions.* Paris, France: International Energy Agency (IEA). Retrieved from https://www.iea.org/reports/the-role-of-critical-minerals-in-clean-energy-transitions

Izvestia News. (2017, 12 1). Electric vertical takeoff aircraft developed in Russia. *Izvestia Newspaper*. Retrieved from https://iz.ru/677679/2017-12-01/elektrosamolet-s-vertikalnym-vzletom-razrabotali-v-rossii

Jaunt Air Mobility LLC. (2021). *Commuting Reimagined*. Retrieved 12 24, 2021, from https://jauntairmobility.com/

Joby Aviation. (2021). *Electric Aerial Ridesharing*. Retrieved 12 24, 2021, from https://www.jobyaviation.com/

KARI. (2021). *Aviation*. Retrieved 12 24, 2021, from Korea Aerospace Research Institute (KARI): https://www.kari.re.kr/eng/sub03_01.do

Kellermann, R., Biehle, T., & Fischer, L. (2020). Drones for parcel and passenger transportation: A literature review. *Transportation Research Interdisciplinary Perspectives, 4*. doi:10.1016/j.trip.2019.100088

Kim, D., Lee, Y., Oh, S., Park, Y., Choi, J., & Park, D. (2021). Aerodynamic analysis and static stability analysis of Manned/unmanned distributed propulsion aircrafts using actuator methods. *Journal of Wind Engineering and Industrial Aerodynamics, 214*, 104648. doi:10.1016/J.JWEIA.2021.104648

Kim, D., Lee, Y., Oh, S., Park, Y., Choi, J., & Park, D. (2021). Aerodynamic analysis and static stability analysis of Manned/unmanned distributed propulsion aircrafts using actuator methods. *Journal of Wind Engineering and Industrial Aerodynamics, 214*. doi:10.1016/j.jweia.2021.104648

Kittyhawk. (2021). *Everyday Flight for Everyone*. Retrieved 12 24, 2021, from https://www.kittyhawk.aero/

Kolodny, L., & Josephs, L. (2021, August 11). Electric Air Taxi Start-up Joby Aviation Surges in Trading on NYSE after SPAC Merger. *CNBC News*. Retrieved from https://www.cnbc.com/2021/08/11/joby-aviation-begins-trading-on-nyse-after-spac-merger.html

Kundu, A. K., Price, M. A., & Riordan, D. (2019). *Conceptual Aircraft Design: An Industrial Approach.* Hoboken, New Jersey: John Wiley & Sons.

Leap Aeronautics. (2021). *The Product Performance*. Retrieved 12 24, 2021, from https://www.leapaero.com/#lastPage

Lee, B., Tullu, A., & Hwang, H. (2020). Optimal design and design parameter sensitivity analyses of an eVTOL PAV in the conceptual design phase. *Applied Sciences (Switzerland), 10*(15). doi:10.3390/app10155112

Lilium GMBH. (2021). *The First Electric Vertical Take-off and Landing Jet*. Retrieved 12 24, 2021, from https://lilium.com/jet

Lineberger, R., Silver, D., & Hussain, A. (2021). *Advanced Air Mobility: Can the United States afford to lose the race?* Retrieved from https://www2.deloitte.com/us/en/insights/industry/aerospace-defense/advanced-air-mobility.html

Micor Technologies. (2021). *Variable Geometry VTOL Aircraft (VAGEV)*. Retrieved 12 24, 2021, from https://micortec.com/hybrid-electric-vtol-aircraft/

MIT. (1997, March 16). *Theory of Flight*. (MIT Department of Aeronautics and Astronautics) Retrieved from https://web.mit.edu/16.00/www/aec/flight.html

Mohamed, N., Al-Jaroodi, J., Jawhar, I., Idries, A., & Mohammed, F. (2020). Unmanned aerial vehicles applications in future smart cities. *Technological Forecasting and Social Change, 153*. doi:10.1016/j.techfore.2018.05.004

Morgan Stanley. (2018). *Flying Cars: Investment Implications of Autonomous Urban Air Mobility.* New York: Morgan Stanley Research. Retrieved from https://www.morganstanley.com/ideas/autonomous-aircraft

Nakamura, H., & Kajikawa, Y. (2018). Regulation and innovation: How should small unmanned aerial vehicles be regulated? *Technological Forecasting and Social Change, 128*. doi:10.1016/j.techfore.2017.06.015

NAS. (2018). *Assessing the Risks of Integrating Unmanned Aircraft Systems into the National Airspace System.* Washington DC: National Academies Press. doi:10.17226/25143

NAS. (2020). *Advancing Aerial Mobility: A National Blueprint.* National Academies of Sciences (NAS). Washington, DC: The National Academies Press. doi:10.17226/25646

NASA. (2021). *Regional Air Mobility: Leveraging Our National Investments to Energize the American Travel Experience.* Washington, D.C.: National Aeronautics and Space Administration (NASA). Retrieved from https://ntrs.nasa.gov/citations/20210014033

Nicola, S. (2021, May 17). Air-Taxi Startup Volocopter Unveils Four-Seater Suburban Shuttle. *Bloomberg*. Retrieved from https://www.bloomberg.com/news/articles/2021-05-17/air-taxi-startup-volocopter-unveils-four-seater-suburban-shuttle

Opener. (2021). *BlackFly Specifications*. Retrieved 12 24, 2021, from https://opener.aero/

Orca Aerosapce. (2021). *Wings on Duty*. Retrieved 12 24, 2021, from https://www.orca-evtol.com/

Overair, Inc. (2021). *Meet Butterfly*. Retrieved 12 24, 2021, from https://overair.com/product/

Palaia, G., Salem, K., Cipolla, V., Binante, V., & Zanetti, D. (2021). A Conceptual Design Methodology for e-VTOL Aircraft for Urban Air Mobility. *Applied Sciences, 11*(22), 10815. doi:10.3390/APP112210815

Pavel, M. (2021). Understanding the control characteristics of electric vertical take-off and landing (eVTOL) aircraft for urban air mobility. *Aerospace Science and Technology*, 107143. doi:10.1016/J.AST.2021.107143

Piccinini, R., Tugnoli, M., & Zanotti, A. (2020). Numerical investigation of the rotor-rotor aerodynamic interaction for evtol aircraft configurations. *Energies, 13*(22). doi:10.3390/en13225995

Ptero Dynamics, Inc. (2021). *Transwing*. Retrieved 12 24, 2021, from https://www.pterodynamics.com/transwing

Pulsiri, N., & Vatananan-Thesenvitz, R. (2021). Drones in Emergency Medical Services: A Systematic Literature Review with Bibliometric Analysis. *International Journal of Innovation and Technology Management, 18*(4). doi:10.1142/S0219877020970019

Sahoo, S., Zhao, X., & Kyprianidis, K. (2020). A review of concepts, benefits, and challenges for future electrical propulsion-based aircraft. *Aerospace, 7*(4), 44. doi:10.3390/aerospace7040044

Samad Aerospace. (2021). *Starling Cargo*. Retrieved 12 24, 2021, from https://www.samadaerospace.com/starling-cargo/

Sigler, D. (2018, 12 24). Things are Looking up in Dubai. *Sustainable Skies*. Retrieved from https://sustainableskies.org/dgworld-prepares-two-drones-small-sky-taxi-sizes/

SkyCab. (2021, September). *Skycab Science. Not Fiction.* Retrieved 12 24, 2021, from https://sky-cab.net/

Sripad, S., & Viswanathan, V. (2021). The promise of energy-efficient battery-powered urban aircraft. *Proceedings of the National Academy of Sciences of the United States of America, 118*(45). doi:10.1073/pnas.2111164118

Terrafugia. (2021). *Aviation Products and Services*. (Geely Technology Group) Retrieved 12 24, 2021, from https://terrafugia.com/

teTra Aviation Corp. (2021). *Mk-5 Specifications*. Retrieved 12 24, 2021, from https://www.tetra-aviation.com/mk-5

Uber Elevate. (2016). *Fast-Forwarding to a Future of On-Demand Urban Air Transportation.* Uber. Retrieved from https://evtol.news/__media/PDFs/UberElevateWhitePaperOct2016.pdf

Vertical Aerospace. (2021). *Faster, Quieter, Greener, Cheaper*. (Vertical Aerospace Group Ltd.) Retrieved 12 24, 2021, from https://vertical-aerospace.com/va-x4/

Vieira, D., Silva, D., & Bravo, A. (2019). Electric VTOL aircraft: the future of urban air mobility (background, advantages and challenges). *International Journal of Sustainable Aviation, 5*(2), 101. doi:10.1504/IJSA.2019.10023187

Voyzon Aerospace. (2021). *Meet VOTO*. Retrieved 12 24, 2021, from http://www.evoto.in/

VTOL Aviation India. (2021). *Abhiyaan_ENU800*. (VTOL Aviation India PVT. Ltd.) Retrieved 12 24, 2021, from https://vtolaviations.com/ABHIYAAN_ENU800.html

Warren, M., Garbo, A., Herniczek, M. T., Hamilton, T., & German, B. (2019). Effects of range requirements and battery technology on electric VTOL sizing and operational performance. *AIAA Scitech 2019 Forum.* San Diego, California: American Institute of Aeronautics and Astronautics, Inc. doi:10.2514/6.2019-0527

Wilke, G. (2020). Aerodynamic Performance of Two eVTOL Concepts. In D. A., H. G., K. E., W. C., T. C., & J. S. (Eds.), *New Results in Numerical and Experimental Fluid Mechanics XII. DGLR 2018. Notes on Numerical Fluid Mechanics and Multidisciplinary Design* (Vol. 142, pp. 392-402). Springer, Cham. doi:10.1007/978-3-030-25253-3_38

Wing Aviation LLC. (2021). *Wing Delivery is Easy to Use*. Retrieved 12 24, 2021, from https://wing.com/how-it-works/

Wingcopter. (2021). *Wingcopter 198*. Retrieved 12 24, 2021, from https://wingcopter.com/wingcopter-198

Wisk Aero LLC. (2021). *Discover the Future of Urban Air Mobility*. Retrieved 12 24, 2021, from https://wisk.aero/aircraft/

Yan, X., Lou, B., Xie, A., Chen, L., & Zhang, D. (2021). A Review of Advanced High-Speed Rotorcraft. *IOP Conference Series: Materials Science and Engineering*, *1102*(1). doi:10.1088/1757-899X/1102/1/012006

Yaprak, Ü., Kılıç, F., & Okumuş, A. (2021). Is the Covid-19 pandemic strong enough to change the online order delivery methods? Changes in the relationship between attitude and behavior towards order delivery by drone. *Technological Forecasting and Social Change, 169*. doi:10.1016/j.techfore.2021.120829

Zheng, X. S., & Rutherford, D. (2021). *Reducing aircraft CO2 emissions: The role of U.S. federal, state, and local policies.* International Council on Clean Transportation (ICCT).

Zong, J., Zhu, B., Hou, Z., Yang, X., & Zhai, J. (2021). Evaluation and comparison of hybrid wing VTOL UAV with four different electric propulsion systems. *Aerospace, 8*(9). doi:10.3390/aerospace8090256